Rudenko, S., Dettmering, D., Esselborn, S., Fagiolini, E., Schöne, T. (2016): Impact of Atmospheric and Oceanic De-aliasing Level-1B (AOD1B) products on precise orbits of altimetry satellites and altimetry results. - *Geophysical Journal International*, *204*, 3, pp. 1695—1702.

DOI: http://doi.org/10.1093/gji/ggv545

Geophysical Journal International

Geophys. J. Int. (2016) **204,** 1695–1702
GJI Gravity, geodesy and tides

doi: 10.1093/gji/ggv545

Impact of Atmospheric and Oceanic De-aliasing Level-1B (AOD1B) products on precise orbits of altimetry satellites and altimetry results

Sergei Rudenko,[1] Denise Dettmering,[2] Saskia Esselborn,[1] Elisa Fagiolini[1] and Tilo Schöne[1]

[1] *Helmholtz Centre Potsdam - GFZ German Research Centre for Geosciences, Department of Geodesy and Remote Sensing, Telegrafenberg, D-*14473 *Potsdam, Germany. E-mail: rudenko@gfz-potsdam.de*
[2] *Deutsches Geodätisches Forschungsinstitut der Technischen Universität München (DGFI-TUM), Arcisstrasse* 21*, D-*80333 *Munich, Germany*

Accepted 2015 December 21. Received 2015 November 16; in original form 2015 August 6

SUMMARY

We have extended backwards from 2001 to 1979 the current release 05 (RL05) of the Gravity Recovery and Climate Experiment (GRACE) Atmospheric and Oceanic De-aliasing Level-1B (AOD1B) product and studied the impact of this and a previous release 04 (RL04) of the AOD1B product on precise orbits of five altimetry satellites (ERS-1, ERS-2, TOPEX/Poseidon, Envisat and Jason-1) for the time span 1991–2012, as compared to the case when no AOD1B product is used. We have found that using AOD1B RL05 product reduces root mean square (RMS) fits of satellite laser ranging (SLR) observations by about 1.0–6.4 per cent, 2-d arc overlaps in radial, cross-track and along-track directions by about 1.3–12.0, 0.3–10.0 and 2.0–10.0 per cent, respectively, for various satellites tested, as compared to the case without AOD1B product. Using AOD1B RL05 product instead of RL04 one reduces SLR RMS fits by 0.1–0.7 per cent, 2-d arc overlaps in radial, cross-track and along-track directions by 0.1–0.6, 0.1–1.3 and 0.2–1.2 per cent, respectively, for the satellite orbits tested. The multi-mission crossover analysis shows that the application of an AOD1B product reduces the scatter of radial errors by 0.4–2.8 per cent for the satellite missions studied. At the regions with the most pronounced changes the use of the AOD1B products improves the consistency between the sea level as measured by the TOPEX and ERS-2 missions and by the Jason-1 and Envisat missions by 5 to 10 per cent (globally by about 2 per cent). The results of our study show that extended AOD1B RL05 product performs better than the AOD1B RL04 and improves orbits of altimetry satellites and consistency of sea level products.

Key words: Satellite geodesy; Sea level change; Time variable gravity.

1 INTRODUCTION

The gravitational attraction of the Earth is the major force acting on an Earth orbiting satellite. This force is usually expressed in the expansion of spherical harmonic coefficients. The up-to-date models of the Earth gravity field, like, for example, EIGEN-6S2 (Rudenko *et al.* 2014), include the static and time variable parts consisting of drifts and periodic, namely, annual and semi-annual variations of geopotential coefficients. However, these variations do not include non-tidal high-frequency atmospheric and oceanic mass variations that should be added to the gravity field model in order to compute orbits of the Earth orbiting satellite with high precision. Atmospheric gravity can be modelled using AGRA (Service of the atmospheric contribution to geopotential) 6-hourly fields (Kalnay *et al.* 1996) and (Petrov & Boy 2004). Atmospheric and oceanic mass variations are provided by Gravity Recovery and Climate Experiment (GRACE) Atmospheric and Oceanic De-aliasing Level-1B (AOD1B) products routinely derived by GFZ German Research Centre for Geosciences and serving as a background model for GRACE as well for a wide range of satellite missions (Flechtner *et al.* 2015). The AOD1B products estimate high-frequency non-tidal mass variations due to short-term (daily and subdaily) mass transport in the atmosphere and oceans, which, if not removed, can alias into monthly gravity solutions derived from such satellite gravity missions as CHAMP (CHAllenging Mini-Satellite Payload), GRACE or GRACE-Follow-On. Cerri *et al.* (2010) studied the contribution of the atmospheric gravity for Jason-1 when using AOD1B and spherical harmonic decomposition of atmospheric pressure over land derived at National Centers for Environmental Prediction (NCEP) and found that the differences between the two are close to 1 mm root mean square (RMS).

In this study, we investigate the impact of AOD1B RL04 and RL05 products and the case when no AOD product is used at all on precise orbits of five altimetry satellites (ERS-1, ERS-2, TOPEX/Poseidon, Envisat and Jason-1) orbiting around the Earth at the altitude of 800–1400 km for the time span 1991–2012. We

show the impact of these products on the RMS fits of observation residuals and 2-d arc overlaps, on the radial orbit components, radial and geographically correlated errors, as well as on the temporal behaviour of geographical patterns.

The paper is organized as follows. Section 2 describes the extended AOD1B RL05 product. Section 3 gives the results of the influence of the RL04 and RL05 of the AOD1B product and the case when no AOD product is used on the observation residuals, arc overlaps and the results of altimetry crossover analysis. Section 4 shows the impact of the AOD1B products on the radial altimeter errors. Section 5 provides the influence of the AOD1B products on sea level estimates. Finally, the conclusions are drawn and the main results are discussed (Section 6).

2 EXTENDED AOD1B RL05 PRODUCT

The AOD1B RL04 and RL05 products are sets of 6-hr spherical harmonic coefficients up to degree and order 100. The later product is updated on a weekly basis and is applied as a background model at the GRACE Science Data System and various other gravity processing centres. The basis of the atmospheric part as well as of the ocean response to atmospheric pressure is the operational analysis of the European Centre for Medium Range Weather Forecast (ECMWF; ECMWF 2007a,b). The basis of the oceanic component is the Ocean Model for Circulation and Tides (OMCT; Thomas *et al.* 2001). The latest RL05 presents an improved OMCT with higher spatial resolution (1° regular grid in RL05 instead of 1.875° in RL04) and improved parametrization (e.g. reduced horizontal eddy viscosity and bottom friction) (Dobslaw *et al.* 2013). The previous RL04 was extended backwards to 1976 in order to be applied in the orbit determination process of satellite missions which were launched before 2001. For the same reason, we have extended in this study the latest release 05 (RL05) backwards from 2001 to 1979, using ERA-Interim (ECMWF Re-Analysis) input data (Dee *et al.* 2011). The extended RL04 product is based on the ECMWF re-analysis data set ERA-40 (Uppala *et al.* 2005). Meanwhile ECMWF produced a new re-analysis data set called ERA-Interim, including an improved atmospheric model and assimilation system which replaced those used in ERA-40. Therefore, we have extracted the input data for the new extended RL05 product from the ERA-Interim archive. The discontinuity due to the change of the input model in 2001 (from re-analysis to operational) has been taken into account. This issue was already considered by the generation of an extended version, back to 1976, of the previous RL04 (Flechtner *et al.* 2008). For the extended RL05, we estimate a correction by generating de-aliasing products for 2001 from both the operational and ERA-Interim archives. For the ERA-Interim case we use the surface pressure approach, while for the operational one we apply the vertical integration of the atmospheric column. In both cases, we subtract a corresponding 2001+2002 mean field (for details see Flechtner *et al.* 2015). A similar approach was applied to correct two discontinuities present in the ECMWF operational analysis data, the so-called 'jumps' in January 2006 and January 2010. Fagiolini *et al.* (2015) generated two additional products called GAE and GAF by comparing de-aliasing products based on the operational analysis and the ERA-Interim data. Both products were provided to the user community and should be added to the already existing AOD1B products in order to correct the two inconsistencies. In the case of the extended AOD1B RL05 product, the correction was added to the data from 1979 till 2001 based on the ERA-Interim data, so no additional action is needed from the user community. The estimated correction (Fig. 1) shows maxima and minima located over high elevation points, consistent with the GAE and GAF spatial features. It presents a range of 340 mm of Equivalent Water Height (EWH) close to the range of the GAF correction (Fagiolini *et al.* 2015). In order to check further the consistency of the new extended AOD1B RL05 product we provide updated plots of 6-hr time series of spherical harmonics 0, 1, 2 degree coefficients for four different data types: atm (variability of the vertical integrated atmosphere), ocn (variability of the OMCT output), glo (variability of the global combination of atmosphere and ocean), and oba (variability of the OMCT ocean bottom pressure). The mean ocn variability must be zero because a mass conserving approach has been used in the RL05 OMCT runs. These plots are available at: http://www-app2.gfz-potsdam.de/pb1/op/grace/results/grav/g007_aod1b_rl05.html, last accessed January 2016. The AOD1B RL05 product can be downloaded from the Information System and Data Center (ISDC) for geoscientific data at the following web link: http://isdc.gfz-potsdam.de/, last accessed January 2016.

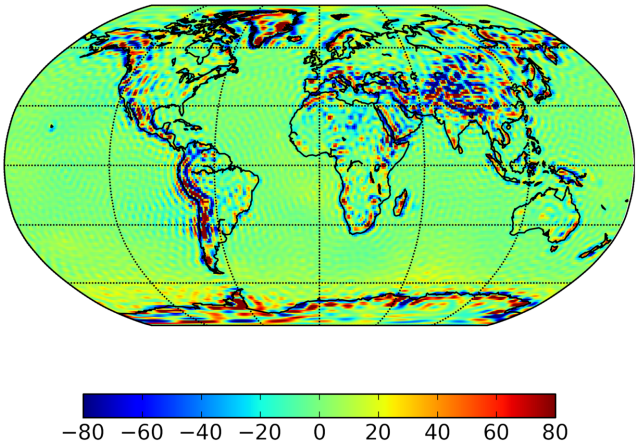

Figure 1. Estimated correction for the AOD1B discontinuity due to the changing ECMWF input data (from ERA-Interim to operational analysis) in mm EWH.

3 EVALUATION OF THE AOD1B PRODUCTS WITH PRECISE ORBIT DETERMINATION OF ALTIMETRY SATELLITES

We have computed precise orbits of altimetry satellites ERS-1 (1991–1996), ERS-2 (1995–2006), TOPEX/Poseidon (1992–2005), Envisat (2002–2012) and Jason-1 (2002–2012) at the time intervals given using the same background models (Rudenko *et al.* 2014), but applying two different releases of the AOD1B product (RL04 and RL05) and no AOD1B data at all. The non-tidal high-frequency atmospheric and oceanic mass variations represented by the AOD1B products are added to the background time variable gravity field model during the precise orbit determination (Flechtner *et al.* 2008). Satellite laser ranging (SLR) measurements available from the International Laser Ranging Service (ILRS; Pearlman *et al.* 2002) and single satellite altimetry crossover (SXO) data computed using the GFZ's Altimeter Data System (ADS Central; Schöne *et al.* 2010) are used to derive ERS-1 orbits. Precise Range And Range-rate Equipment (PRARE) measurements available from GFZ are used additionally for ERS-2. The orbits of TOPEX/Poseidon, Envisat and Jason-1 are derived using SLR and DORIS (Doppler

Table 1. The mean values of RMS fits of observations and 2-d arc overlaps for ERS-1 obtained using no AOD, AOD1B RL04 and RL05 products.

AOD product	SLR (cm)	SXO (cm)	Radial arc overlap (cm)	Cross-track overlap (cm)	Along-track overlap (cm)
No AOD	2.183	4.828	1.894	17.199	12.479
RL04	2.150	4.788	1.836	17.143	12.140
RL05	2.138	4.778	1.824	16.916	12.074

Table 2. The mean values of RMS fits of observations and 2-d arc overlaps for TOPEX/Poseidon obtained using no AOD, AOD1B RL04 and RL05 products.

AOD product	SLR (cm)	DORIS (mm s^{-1})	Radial arc overlap (cm)	Cross-track overlap (cm)	Along-track overlap (cm)
No AOD	2.072	0.4799	1.030	6.548	3.700
RL04	2.022	0.4797	1.023	6.535	3.593
RL05	2.012	0.4796	1.016	6.525	3.551

Orbitography and Radiopositioning Integrated by Satellite) observations available from the International DORIS Service (IDS; Willis *et al.* 2010). Tables 1–5 provide the mean values of RMS fits of SLR, SXO, DORIS, PRARE range and PRARE Doppler observations, as well as 2-d orbital arc overlaps in radial, cross-track and along-track directions for the orbits of each satellite computed using no AOD data, AOD1B RL04 and RL05 products. The orbit tests definitely show (Tables 1–5) that the mean values of RMS fits of observations and 2-d arc overlaps improve for all five satellites, when one of the AOD1B products (either RL04 or RL05) is used, as compared to the case without AOD product. Thus, the mean values of RMS fits of SLR observations reduce by 2.1, 3.4, 6.4, 2.9 and 1.0 per cent for ERS-1, ERS-2, Envisat, TOPEX/Poseidon and Jason-1, respectively, for comparisons of results obtained with AOD1B RL05 and without AOD products. Using the AOD1B RL05 product instead

Table 3. The mean values of RMS fits of observations and 2-d arc overlaps for Envisat obtained using no AOD, AOD1B RL04 and RL05 products.

AOD product	SLR (cm)	DORIS (mm s^{-1})	Radial arc overlap (cm)	Cross-track overlap (cm)	Along-track overlap (cm)
No AOD	1.379	0.4291	0.456	2.095	1.312
RL04	1.301	0.4286	0.401	1.880	1.192
RL05	1.291	0.4286	0.401	1.886	1.181

Table 4. The mean values of RMS fits of observations and 2-d arc overlaps for Jason-1 obtained using no AOD, AOD1B RL04 and RL05 products.

AOD product	SLR (cm)	DORIS (mm s^{-1})	Radial arc overlap (cm)	Cross-track overlap (cm)	Along-track overlap (cm)
No AOD	1.524	0.3574	0.775	4.362	2.165
RL04	1.511	0.3573	0.761	4.349	2.126
RL05	1.509	0.3573	0.758	4.340	2.120

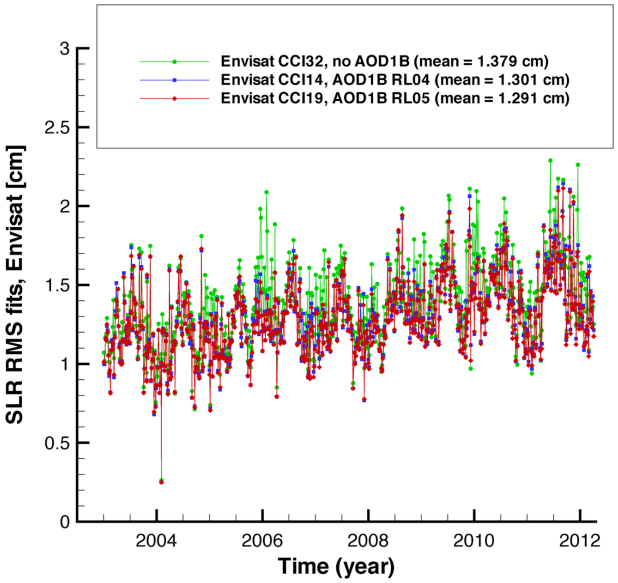

Figure 2. RMS fits of SLR observations for Envisat orbits computed using no AOD, AOD1B RL04 and RL05 products.

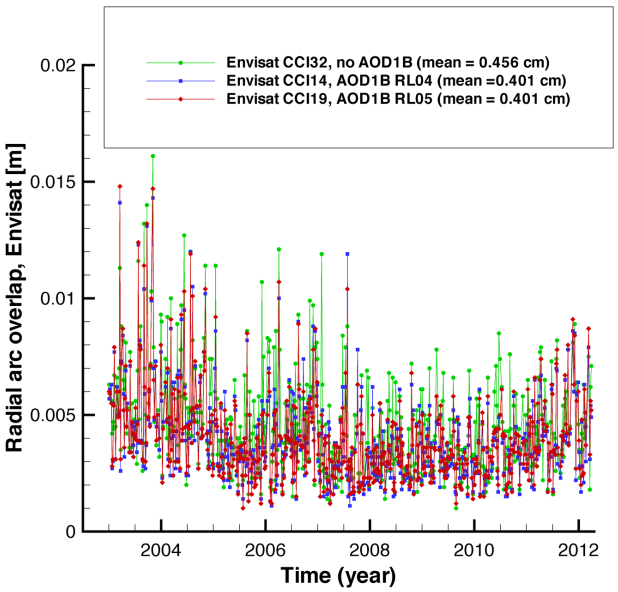

Figure 3. Two-day radial arc overlaps for Envisat orbits computed using no AOD, AOD1B RL04 and RL05 products.

of the AOD1B RL04 product reduces the mean values of RMS fits of SLR observations by 0.6, 0.6, 0.7, 0.5 and 0.1 per cent for ERS-1, ERS-2, Envisat, TOPEX/Poseidon and Jason-1, respectively. The temporal behaviour of RMS fits of SLR observations and 2-d radial arc overlaps for Envisat orbits computed using no AOD, AOD1B RL04 and RL05 data are exemplary shown in Figs 2 and 3. GFZ internal orbit names (CCI*) are provided for the reference. Tables 1–5 indicate that the mean values of the RMS fits of SLR

Table 5. The mean values of RMS fits of observations and 2-d arc overlaps for ERS-2 obtained using no AOD, AOD1B RL04 and RL05 products.

AOD product	SLR (cm)	SXO (cm)	PRARE range (cm)	PRARE Doppler (mm s^{-1})	Radial arc overlap (cm)	Cross-track overlap (cm)	Along-track overlap (cm)
No AOD	1.744	4.162	3.469	0.3945	1.889	7.502	10.966
RL04	1.696	4.099	3.456	0.3931	1.836	7.114	10.690
RL05	1.685	4.095	3.438	0.3916	1.834	7.447	10.670

Table 6. The mean values of the RMS and mean of crossover differences based on ERS-1 and ERS-2 orbits derived using no AOD, AOD1B RL04 and RL05 products. The crossover statistics are computed over 198 weeks from 1992 July 9 to 1996 May 30 for ERS-1 and 415 weeks from 1995 May 15 till 2003 June 16 for ERS-2.

AOD product	RMS of ERS-1 crossover differences (cm)	Mean of ERS-1 crossover differences (cm)	RMS of ERS-2 crossover differences (cm)	Mean of ERS-2 crossover differences (cm)
No AOD	6.116	0.080	6.353	0.008
RL04	6.090	0.116	6.347	0.032
RL05	6.079	0.082	6.342	0.010

observations are about 2.1 cm for ERS-1, 1.7 cm for ERS-2, 2.0 cm for TOPEX/Poseidon, 1.3 cm for Envisat and 1.5 cm for Jason-1 using the AOD1B RL05 product. Tables 2–4 show that the mean values of the RMS fits of DORIS measurements are about 0.48, 0.43 and 0.36 mm s^{-1} for TOPEX/Poseidon, Envisat and Jason-1, respectively. The internal consistency of the satellite orbits in the radial direction (most important for altimetric application) provided by the mean values of the radial arc overlap is 1.8 cm for ERS-1 and ERS-2, 1.0 cm for TOPEX/Poseidon, 0.4 cm for Envisat and 0.8 cm for Jason-1. One can see that Envisat orbit based on using additionally to SLR also DORIS measurements has about 4.5 times better internal orbit accuracy in the radial direction, as compared to the orbits of satellites computed using just SLR and single-satellite altimeter crossover data (like ERS-1 and ERS-2 located at the same altitude).

Single-satellite altimetry crossover analysis of ERS-1 orbits shows 0.43 and 0.60 per cent reduction of the RMS of crossover differences when using AOD1B RL04 and AOD1B RL05, respectively, as compared to the case without AOD product (Table 6). The mean of altimetry crossover differences is smaller when AOD1B RL05 is used, as compared when AOD1B RL04 is used.

4 INFLUENCE OF AOD1B PRODUCTS ON RADIAL AND GEOGRAPHICALLY CORRELATED ALTIMETER ERRORS

In order to evaluate the accuracy and intermission consistency of the different orbit solutions (which are based on different AOD1B products) a global multi-mission crossover analysis is conducted. This method provides time series of radial errors for all missions. Even if orbit errors and especially single components of orbit errors (such as AOD1B effects) are only one part of the radial errors the comparison of the three different solutions computed without changing other parameters can reveal the effect of different AOD1B products to the radial errors of altimetry missions.

The main idea behind the multi-mission crossover analysis (MMXO) is to detect inconsistencies between the altimeter missions by comparing independent measurements of the same sea surface. The algorithm used within this paper is documented in Bosch *et al.* (2014) and provides not only global mean range biases but also radial errors for each altimeter measurement under the assumption that the TOPEX mission provides offset-free observations (range bias of zero). The distribution of the influences on different missions is done automatically by means of variance component estimation. The basic outputs of the MMXO are time series of radial errors for each mission participating in the analysis (including the reference mission TOPEX). These radial errors can be analysed in detail in a post-processing step in order to identify systematic patterns (e.g. geographically correlated errors) or other systematic and random errors. Detailed information on the method can be found in Bosch *et al.* (2014) and the results from MMXO for the calibration of single missions are given, for example, in Dettmering & Bosch (2010) and Dettmering *et al.* (2015).

Table 7. Scatter of radial error over the whole mission lifetimes (including extended mission phases). For the two AOD1B versions, the improvement in per cent with respect to the AOD1B-free version (first column) is given in brackets (negative values indicate improvements).

Mission	No AOD1B (mm)	With AOD1B RL04 (mm)	With AOD1B RL05 (mm)
ERS-1	18.909	18.383 (−2.8 per cent)	18.434 (−2.5 per cent)
ERS-2	25.405	25.313 (−0.4 per cent)	25.309 (−0.4 per cent)
Envisat	17.907	17.662 (−1.4 per cent)	17.602 (−1.7 per cent)
TOPEX	16.186	15.928 (−1.6 per cent)	15.862 (−2.0 per cent)
Jason-1	15.932	15.735 (−1.2 per cent)	15.712 (−1.4 per cent)

Table 8. Percentage of 10-d periods without improvement when using AOD1B product.

	ERS-1 (per cent)	ERS-2 (per cent)	Envisat (per cent)	TOPEX (per cent)	Jason-1 (per cent)
RL04 wrt no AOD	37.0	33.9	15.8	30.2	30.7
RL05 wrt no AOD	23.7	28.8	13.0	21.0	26.3

It is important to understand that the radial errors provided by MMXO do not only comprise orbital errors but also include effects coming from the altimeter systems themselves and from geophysical corrections applied to the data. However, since only differences between the different solutions based on different orbits are analysed and all other data sets including the MMXO parameters remain identical the differences can be explicitly assigned to orbit effects.

4.1 Influence of AOD1B products on radial errors of altimeter measurements

Whereas the radial errors themselves show only minor differences when comparing results from the different orbit solutions (maximal 0.2 per cent change), one can see significant influence on the scatter of radial errors over the mission lifetimes. Table 7 summarizes the values for all missions and three orbit solutions based on different AOD1B products. The application of an AOD1B product reduces the scatter of radial errors by up to 2.8 per cent. With the exception of ERS-1 the RL05 product slightly outperforms the older version. Even if the scatter of radial errors is notably influenced by the choice of AOD product, it is obvious that the main parts of the errors are due to other influences.

Although the scatter over the whole mission lifetimes reduces significantly when using AOD1B corrections there exists some time periods without improvements. We investigated the scatter for 10-d subsets of radial errors and found that for 16–37 per cent of the time no reduction in the scatter of radial errors is detected when applying the AOD1B RL04 product. These values can be reduced to 13–29 per cent with RL05 (*cf.* Table 8). Although a systematic time-dependent behaviour over the mission lifetimes is not detectable there is still room for further improvement.

4.2 Influence of AOD1B products on geographically correlated errors

In order to investigate the geographical distribution of the radial errors estimated by MMXO geographically correlated errors (GCE)

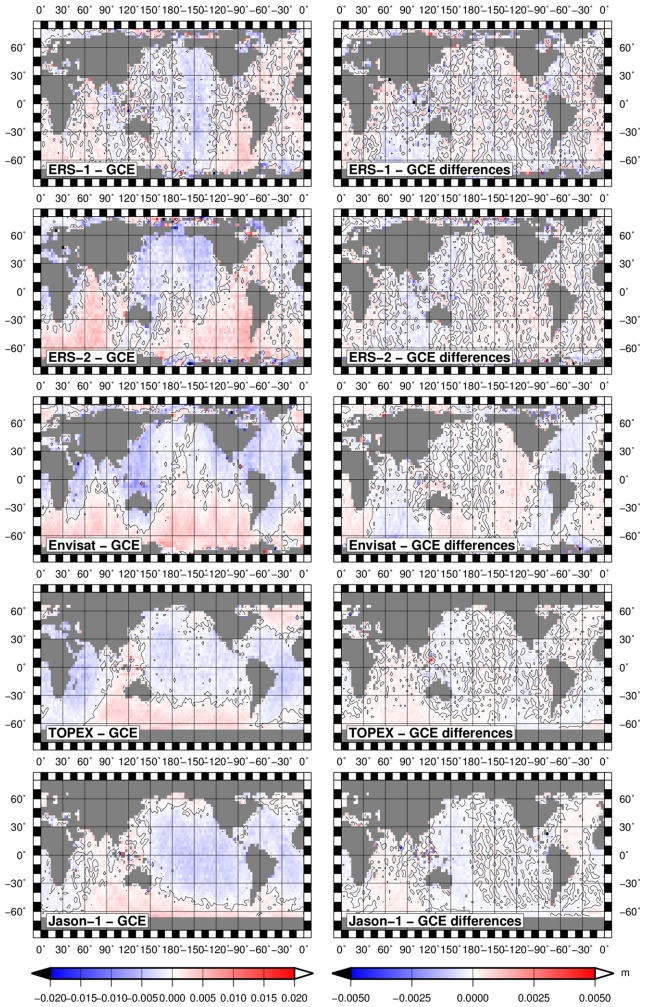

Figure 4. Geographically correlated errors for all five missions based on the orbits computed with AOD1B R05 (left-hand side) and the differences between this solution and the solution without applying any AOD1B product (right-hand side).

are computed. For this purpose, the radial errors of each mission are separated in its mean and variable component by averaging the radial errors separately for ascending and descending ground tracks on a $3^\circ \times 3^\circ$ grid. By averaging the mean values of corresponding grid cells a gridded estimate of the GCE can be derived. This method is explained in more detail in Bosch *et al.* (2014). Since the GCE are computed based on the radial errors from MMXO, the GCE represent the sum of all influences where orbit effects are only one part.

The application of AOD1B changes the GCE notably. From the right column of Fig. 4, it can be seen that the GCE differences reach a maximum of about 5 mm. In most areas, the values stay below 1 mm and the number of grid cells with values larger than 1 mm range between 1 per cent for Jason-1 and 7 per cent for ERS-1. Larger structures cannot be easily detected. Table 9 summarizes the scatter of GCE, which is between 2 and 3.5 mm depending on mission and solution. The RL05 yields a maximal improvement of about 2 per cent for Jason-1. However, there is no clear indication that RL04 is inferior to RL05. For ERS-1 the AOD1B R04 product even enlarges the GCE. Looking at Fig. 4, similarities between the ESA missions (ERS-1, ERS-2, Envisat) on the one hand and NASA/CNES missions (TOPEX and Jason-1) on the other hand are

Table 9. Scatter of GCE over the whole mission lifetimes (including extended mission phases). For the two AOD1B versions, the changes in per cent with respect to the orbits without AOD1B are given in brackets (negative values indicate improvements).

Mission	No AOD1B (mm)	With AOD1B RL04 (mm)	With AOD1B RL05 (mm)
ERS-1	2.565	2.624 (+2.3 per cent)	2.531 (−1.3 per cent)
ERS-2	3.452	3.375 (−2.2 per cent)	3.403 (−1.4 per cent)
Envisat	2.941	2.921 (−0.7 per cent)	2.901 (−1.4 per cent)
TOPEX	2.049	2.013 (−1.7 per cent)	2.016 (−1.6 per cent)
Jason-1	2.034	2.029 (−0.2 per cent)	1.989 (−2.2 per cent)

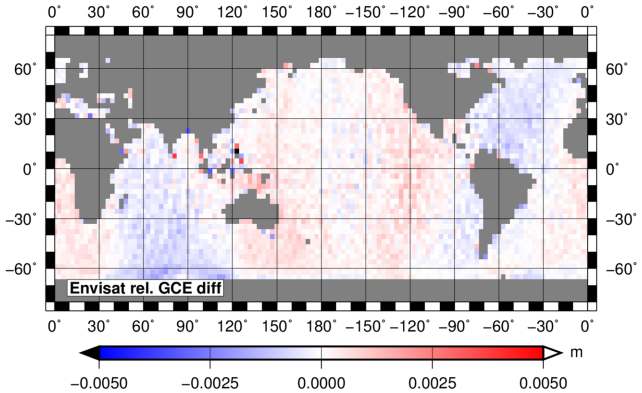

Figure 5. Differences of geographically correlated error differences (without AOD1B minus RL05) between Envisat and Jason-1.

visible. Moreover, the NASA/CNES missions seem to be reversed from ESA missions. Thus, the improvements by AOD1B RL05 (right-hand side of the figure) depend on the orbit itself. Building the relative differences of the ESA missions with respect to TOPEX or Jason-1 (e.g. the differences between the plots on the right-hand side of Fig. 4), for all three missions similar patterns occur showing maximal values of about 5 mm and standard deviations around 0.5 mm. For 99.5 per cent of the area the differences are less than 1.5 mm. This is illustrated in Fig. 5 for Envisat with respect to Jason-1. All other ESA-NASA/CNES mission combinations look similar and show identical geographic pattern. The application of the AOD1B RL05 product reduces the intermission inconsistencies by 2.4 per cent from 0.22 ± 3.02 mm to 0.20 ± 2.94 mm (mean differences).

4.3 Influence of AOD1B products on temporal behaviour of geographic pattern

The GCE only show the mean behaviour without temporal variations. In order to detect and analyse potential time-dependent effects the radial errors are analysed in a different way. First, they are separated to 10-d time periods. Then, the radial errors are used to estimate mean range bias r, as well as centre-of-origin shifts x, y, and z for each mission and each 10-d period following (Bosch *et al.* 2014).

The x- and z-components of the shifts do not show any systematics, however, the y-component representing the East-West shift reveals some annual oscillation. Fig. 6 shows the differences of y between the solutions without AOD1B product and with AOD1B RL05 for Envisat with respect to Jason-1. A clear annual behaviour is visible. The analysis has been done based on the relative product since the separation of the effect between the missions (and

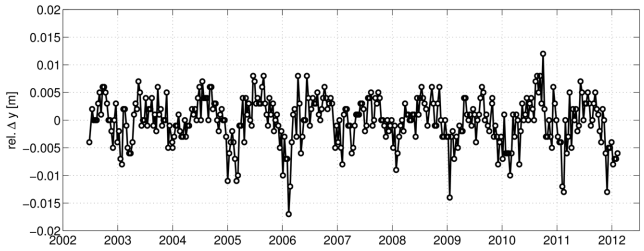

Figure 6. Envisat relative centre-of-origin differences (y-component) due to AOD1B product with respect to Jason-1.

especially the reference mission) by MMXO is not always reliable (Dettmering & Bosch 2010).

This analysis indicates that the geographic pattern visible in Fig. 5 changes over time with annual variations.

5 EFFECTS OF THE AOD1B PRODUCTS ON SEA LEVEL ESTIMATES

In order to quantify the changes in sea level height arising from the use of AOD products for the precise orbit determination (POD) we analyse the differences between the radial orbit components for no AOD and AOD1B RL05 and between AOD1B RL05 and RL04. The radial orbit components presented here map directly to the derived sea surface heights. The corresponding analyses are performed for all five missions.

5.1 Sea level height changes related to the AOD1B products

Radial orbit differences are calculated along-track for the times of the altimeter range measurements (about 1 Hz). Afterwards the radial orbit differences are interpolated to a $1^\circ \times 1^\circ$ grid every 35 d for the ERS-1, ERS-2 and Envisat missions and every 10 d for the TOPEX and Jason-1 missions. From the gridded time series of the radial differences regional values of mean, RMS and annual cycle are calculated. At first, the geographical patterns of the radial changes between the no AOD and AOD1B RL05 are analysed. Whereas the mean differences between the two orbits are less than 2 mm, the RMS values reach locally up to 7 mm for the TOPEX, up to 6 mm for the ERS-1 and ERS-2 and up to 5 mm for the Envisat and Jason-1 missions. For all missions, the RMS values of the orbit differences peak over two centres—close to Central America and Australia. An analysis of the temporal variability exhibits mainly annual signals with amplitudes of up to 7 mm. In addition, small changes of the regional sea level trends can be observed. They range for most missions around ± 0.2 mm yr^{-1}. An exception is the ERS-1 mission where the differences between the AOD1B RL05 and the no AOD orbits reach up to ± 1 mm yr^{-1}. The geographical patterns of annual amplitudes and phases for the ERS-1 and TOPEX orbits are shown in Fig. 7. The annual phase between the two missions is shifted by 180°. The annual signal of the ERS-2 and Envisat missions is very similar to the one of ERS-1, the annual signal for the Jason-1 mission resembles the one from TOPEX. This is in accordance with the results presented in Section 4.

5.2 Intermission consistency

To check the performance of the different orbits solutions the consistency of sea level data from the ERS-2 and TOPEX missions and from the Envisat and Jason-1 missions is evaluated. The focus is on

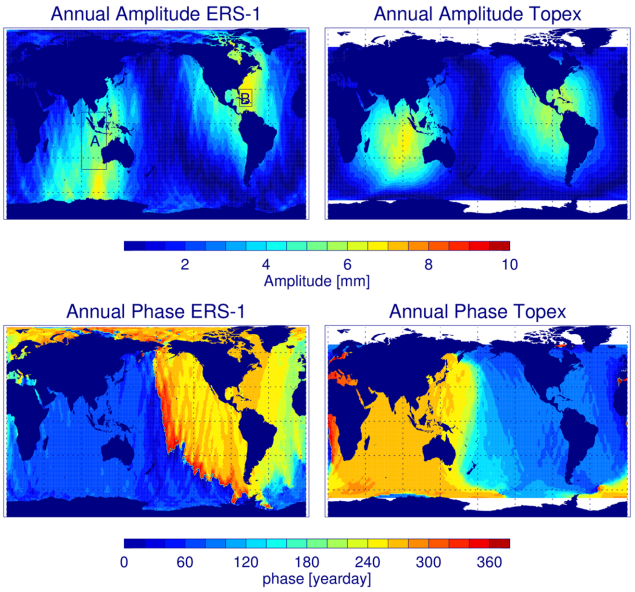

Figure 7. Annual amplitudes (top) and phases (bottom) of the radial orbit differences of ERS-1 (left) and TOPEX (right) orbits computed using AOD1B RL05 and no AOD product. In the upper left, two regions (A and B) are marked which are used to study intermission differences.

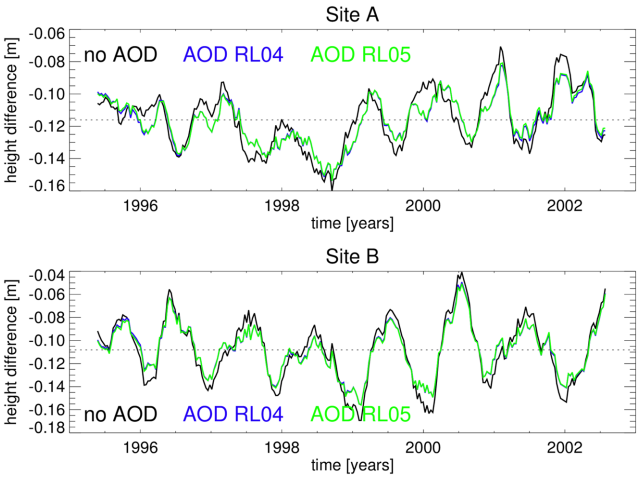

Figure 8. Time series of sea level differences between TOPEX and ERS-2. The sea level is averaged over the two areas showing maximum changes denoted as site A: 40°S–10°N, 90°–120°E and site B: 15°–30°N, 65°–80°W. The differences are calculated for all three orbits (black: no AOD; blue: AOD1B RL04; green: AOD1B RL05). A 70-d box-car filter is applied.

the two centres where maximum variability and annual amplitudes are observed. In the following those regions are denoted as site A (40°S–10°N, 90°–120°E) and site B (15°–30°N, 65°–80°W). For these regions 10-d time series of sea level anomalies (i.e. relative to the mean sea surface height model CLS01; Hernandez & Schaeffer 2001) averaged over site A and site B are calculated for all three orbit solutions. The analysed periods span 1995 May 20 to 2002 July 31 for TOPEX and ERS-2 and 2002 October 28 to 2012 March 7 for Jason-1 and Envisat. The data are processed using the GFZ's Altimeter Data System (ADS Central) (Schöne *et al.* 2010) using similar correction models but no intermission bias. The low-pass filtered differences between the TOPEX and ERS-2 missions for site A and B models are shown in Fig. 8 for all three orbit solutions. Even though the intermission sea level differences are dominated by

Table 10. RMS of 'TOPEX minus ERS-2' and 'Jason-1 minus Envisat' sea level differences for site A: 40°S–10°N, 90°–120°E and site B: 15°–30°N, 65°–80°W. The RMS values are calculated for all three orbits and for the periods 1995 May 20 to 2002 July 31 and 2002 October 28 to 2012 March 7.

	No AOD (mm)	AOD RL04 (mm)	AOD RL05 (mm)
Site A (TOPEX - ERS-2)	27.0	24.2	24.2
Site A (Jason-1 - Envisat)	21.6	20.4	20.4
Site B (TOPEX - ERS-2)	41.6	36.8	36.6
Site B (Jason-1 - Envisat)	27.8	25.5	25.5

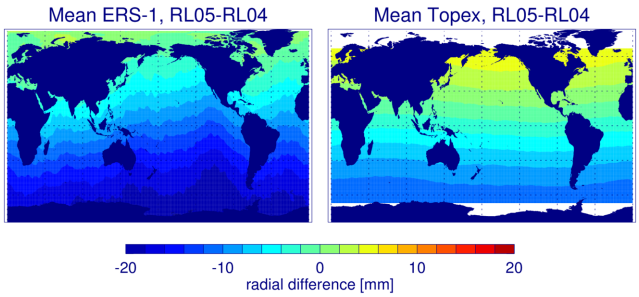

Figure 9. Geographical distribution of the temporal mean of the radial orbit differences of ERS-1 and TOPEX orbits computed using AOD1B RL05 and RL04 products.

other errors (e.g. ionospheric corrections) the consistency between the missions is improved when applying the AOD products for POD. The RMS values of the sea level differences for both sites and all three orbits are given in Table 10. These values fit well to the global analysis based on radial errors, *cf.* Fig. 5. At sites A and B where the largest radial orbit changes occur the intermission differences are diminished by about 10 per cent for the TOPEX and ERS-2 missions and by more than 5 per cent for the Envisat and Jason-1 missions when applying one of the AOD products.

5.3 Differences between different AOD1B releases

The mean radial differences of the orbits derived using the AOD1B RL04 and RL05 corrections are rather small. However, for ERS-1 and TOPEX there are mean differences of the radial orbit component when upgrading the AOD1B release (Fig. 9). In addition to a bias between the orbits there is evidence for an apparent north–south shift of the centre-of-origin of the orbits. Further analyses show that these differences are introduced with the use of the AOD1B RL04 data and disappear again with the use of the RL05 data. Thus, using the RL04 for orbit computations is not recommended since it might lead to sea level changes up to 1 cm in polar regions for TOPEX and ERS-1.

6 DISCUSSION AND CONCLUSIONS

We have successfully extended backwards from 2001 to 1979 the latest release 05 of the AOD1B model. The new time series are stable and free from discontinuities caused by the changes in the input model. The implication of the AOD1B RL04 and RL05 products on precise orbit determination of five different altimetry satellites has been investigated. We have found that using AOD1B RL05 product reduces RMS fits of SLR observations by about 1.0–6.4 per cent, 2-d arc overlaps in radial, cross-track and along-track directions by about 1.3–12.0, 0.3–10.0 and 2.0–10.0 per cent, respectively, for various satellites tested, as compared to the case without AOD1B product. Using AOD1B RL05 product instead of RL04 one reduces SLR RMS fits by 0.1–0.7 per cent, 2-d arc overlaps in radial, cross-track and along-track directions by 0.1–0.6, 0.1–1.3 and 0.2–1.2 per cent, respectively, for the satellite orbits tested.

The MMXO shows that the application of an AOD1B product reduces the scatter of radial errors by 0.4–2.8 per cent for the satellite missions used in this study. With the exception of ERS-1 the AOD1B RL05 product brings an additional (0.2–0.4 per cent) reduction of the scatter of radial errors, as compared to the AOD1B RL04 product. The scatter of the geographically correlated errors reduces by 0.2–2.2 per cent for the four satellites tested, but ERS-1, for which it increases by 2.3 per cent, when using the AOD1B RL04 product. However, application of the AOD1B RL05 reduces the scatter of the geographically correlated errors by 1.3–2.2 per cent for all five satellites using the AOD1B RL05 product, as compared to the case, when no AOD1B product is used.

In order to quantify the changes in sea level height arising from the use of AOD products for the POD the gridded differences between the radial orbit components of the three orbit versions are analysed. The major changes occur between the AOD1B RL05 and the no AOD orbits. The RMS values of the differences reach maximum values between 7 and 5 mm depending on the mission. The observed difference patterns are large-scale and seem to resemble centre-of-origin shifts, mainly with annual frequency and amplitudes up to 7 mm, which are in antiphase between the TOPEX/Jason-1 missions and the ESA missions. Similar difference patterns have been observed before and could be related to changes in the gravity-field model used to estimate the orbits (e.g. Rudenko *et al.* 2014; Esselborn *et al.* 2015).

At the regions with the most pronounced changes the use of the AOD products improves the consistency between the sea level as measured by the TOPEX and the ERS-2 missions and by the Jason-1 and Envisat missions by 5 to 10 per cent (globally by about 2 per cent). For most missions the drifts of the difference of the radial orbit components are less than 0.25 mm yr^{-1}. However, for the ERS-1 mission the use of the AOD products leads to changes of the regional trends of up to 1 mm yr^{-1}, and the update of the RL04 to the RL05 version leads to changes of up to 0.5 mm yr^{-1}. We could not validate one or the other trend but this is a further indication that regional sea level trends from ERS-1 might not be sufficiently constrained for the use for long term climate sea level series. Using AOD1B RL04 for orbit computations is not recommended, since it might lead to sea level changes up to 1 cm in polar regions for TOPEX and ERS-1.

The results of our study show that the AOD1B RL05 product performs better than the AOD1B RL04 and improves orbits of altimetry satellites and consistency of sea level products.

ACKNOWLEDGEMENTS

This study was performed within the ESA Climate Change Initiative Sea Level Phase 2 project, 'Consistent Estimate of Ultra-High Resolution Earth Surface Gravity Data (UHR-GravDat)' project funded by the German Research Foundation (DFG) and under grant 03F0654A of the German Ministry for Education and Research (BMBF). SLR and DORIS data available from ILRS and IDS were used in this research. The authors are grateful to two anonymous Reviewers for their valuable comments that improved the paper.

REFERENCES

Bosch, W., Dettmering, D. & Schwatke, C., 2014. Multi-mission cross-calibration of satellite altimeters: constructing a long-term data record for global and regional sea level change studies, *Remote Sens.,* **6**(3), 2255–2281.

Cerri, L. *et al.*, 2010. Precision Orbit Determination Standards for the Jason Series of Altimeter Missions, *Mar. Geod.,* **33**(S1), 379–418.

Dee, D.P. *et al.*, 2011. The ERA-Interim reanalysis: configuration and performance of the data assimilation system, *Q. J. R. Meteorol. Soc.,* **137,** 553–597.

Dettmering, D. & Bosch, W., 2010. Global Calibration of Jason-2 by Multi-Mission Crossover Analysis, *Mar. Geod.,* **33**(Suppl. 1), 150–161.

Dettmering, D., Schwatke, C. & Bosch, W., 2015. Global calibration of SARAL/AltiKa using multi-mission sea surface height crossovers, *Mar. Geod.,* **38**(Suppl. 1), 206–218.

Dobslaw, H., Flechtner, F., Bergmann-Wolf, I., Dahle, C., Dill, R., Esselborn, S., Sasgen, I. & Thomas, M., 2013. Simulating high-frequency atmosphere-ocean mass variability for de-aliasing of satellite gravity observations: AOD1B RL05, *J. geophys. Res.,* **118**(7), 3704–3711.

ECMWF, 2007a. IFS Documentation - Cy31r1. Part III: Dynamics and numerical procedures.

ECMWF, 2007b. IFS Documentation - Cy31r1. Part IV: Physical processes.

Esselborn, S., Schöne, T. & Rudenko, S., 2015. Impact of time variable gravity on annual sea level variability from altimetry, in *International Association of Geodesy Symposia 2015,* Springer International Publishing Switzerland 2015, doi:10.1007/1345_2015_103.

Fagiolini, E., Flechtner, F., Horwath, M. & Dobslaw, H., 2015. Correction of inconsistencies in ECMWFB's operational analysis data during de-aliasing of GRACE gravity models, *Geophys. J. Int.,* **202**(3), 2150–2158.

Flechtner, F., Thomas, M. & König, R., 2008. A long-term model for non-tidal atmospheric and oceanic mass redistributions and its implications on LAGEOS-derived solutions of Earths oblateness, *Scientific Technical Report STR08/12, GeoForschungsZentrum Potsdam*, doi:10.2312/GFZ.b103-08123.

Flechtner, F., Dobslaw, H. & Fagiolini, E., 2015. AOD1B product description document for product release 05 (Rev. 4.3), Technical Report, GFZ German Research Center for Geosciences, Potsdam, Available at: http://www.gfz-potsdam.de/fileadmin/gfz/sec12/pdf/GRACE/AOD1B/AOD1B_20150423.pdf, last accessed November 2015.

Hernandez, F. & Schaeffer, P., 2001. *The CLS01 Mean Sea Surface: A Validation with the GSFC00 Surface*, CLS Ramonville.

Kalnay, E. *et al.*, 1996. NCEP/NCAR 40-year reanalysis project, *Bull. Am. Meteorol. Soc.,* **77**(3), 437–471.

Pearlman, M.R., Degnan, J.J. & Bosworth, J.M., 2002. The International Laser Ranging Service, *Adv. Space Res.,* **30**(2), 135–143.

Petrov, L. & Boy, J.P., 2004. Study of the atmospheric pressure loading signal in very long baseline interferometry observations, *J. geophys. Res.,* **109,** B03405, doi:10.1029/2003JB002500.

Rudenko, S. *et al.*, 2014. Influence of time variable geopotential models on precise orbits of altimetry satellites, global and regional mean sea level trends, *Adv. Space Res.,* **54,** 92–118.

Schöne, T., Esselborn, S. & Rudenko, S., 2010. Radar altimetry derived sea level anomalies - the benefit of new orbits and harmonization, in *System Earth via Geodetic-Geophysical Space Techniques,* pp. 317–324, eds Flechtner, F., Gruber, T., Güntner, A., Mandea, M., Rothacher, M., Schöne, T. & Wickert, J., Springer.

Thomas, M., Suendermann, J. & Maier-Reimer, E., 2001. Consideration of ocean tides in an OGCM and impacts on subseasonal to decadal polar motion excitation, *Geophys. Res. Lett.,* **28,** 2457–2460.

Uppala, S.M. *et al.*, 2005. The ERA-40 re-analysis, *Q. J. R. Meteorol. Soc.,* **131,** 2961–3012.

Willis, P. *et al.*, 2010. The International DORIS Service, toward maturity, *Adv. Space Res.,* **45**(12), 1408–1420.